

Article

Syngas Production from Combined Steam Gasification of Biochar and a Sorption-Enhanced Water–Gas Shift Reaction with the Utilization of CO₂

Supanida Chimpae ¹, Suwimol Wongsakulphasatch ¹, Supawat Vivanpatarakij ^{2,*}, Thongchai Glinrun ³, Fasai Wiwatwongwana ⁴, Weerakanya Maneeparakorn ⁵ and Suttichai Assabumrungrat ⁶

¹ Department of Chemical Engineering, Faculty of Engineering, King Mongkut's University of Technology North Bangkok, Bangkok 10800, Thailand; s5601031620023@email.kmutnb.ac.th (S.C.); suwimol.w@eng.kmutnb.ac.th (S.W.)

² Energy Research Institute, Chulalongkorn University, Phayathai Road, Wang Mai, Phatumwan, Bangkok 10330, Thailand

³ Department of Petrochemical and Environmental Engineering, Faculty of Engineering, Pathumwan Institute of Technology, Rama 1 Road, Wang Mai, Phatumwan, Bangkok 10330, Thailand; thongchai@pit.ac.th

⁴ Department of Advanced Manufacturing Technology, Faculty of Engineering, Pathumwan Institute of Technology, 833 Rama 1 Road, Wangmai, Pathumwan, Bangkok 10330, Thailand; fasiaw227@gmail.com

⁵ National Nanotechnology Center (NANOTEC), National Science and Technology Development Agency (NSTDA), Pathum Thani 12120, Thailand; weerakanya@nanotec.or.th

⁶ Center of Excellence in Catalysis and Catalytic Reaction Engineering, Department of Chemical Engineering, Faculty of Engineering, Chulalongkorn University, Bangkok 10330, Thailand; Suttichai.A@chula.ac.th

* Correspondence: supawat.v@chula.ac.th

Received: 24 April 2019; Accepted: 1 June 2019; Published: 7 June 2019



Abstract: This research aims at evaluating the performance of a combined system of biochar gasification and a sorption-enhanced water–gas shift reaction (SEWGS) for synthesis gas production. The effects of mangrove-derived biochar gasification temperature, pattern of combined gasification and SEWGS, amount of steam and CO₂ added as gasifying agent, and SEWGS temperature were studied in this work. The performances of the combined process were examined in terms of biochar conversion, gaseous product composition, and CO₂ emission. The results revealed that the hybrid SEWGS using one-body multi-functional material offered a greater amount of H₂ with a similar amount of CO₂ emissions when compared with separated sorbent/catalyst material. The gasification temperature of 900 °C provided the highest biochar conversion of ca. 98.7%. Synthesis gas production was found to depend upon the amount of water and CO₂ added and SEWGS temperature. Higher amounts of H₂ were observed when increasing the amount of water and the temperature of the SEWGS system.

Keywords: gasification; sorption-enhanced water–gas shift; multi-functional material

1. Introduction

Synthesis gas or syngas, which is composed mainly of H₂ and CO, can be applied for various downstream processes, e.g., electricity generation or chemical production [1–3]. The conversion of biomass by thermochemical processes such as gasification or pyrolysis has been extensively used to produce syngas and is recognized as an environmental-friendly technique as it is carbon-neutral [4]. The thermochemical process can be performed using different operating conditions, i.e., gasifying agent, temperature, pressure, etc., which could yield different amounts and compositions of syngas [5–7]. In addition, strategic techniques have also been applied for upgrading syngas, i.e., integrated gas–solid

simultaneous gasification and catalytic reforming [8], a two-stage pyrolysis-reforming system [9], a two-stage gasification-reforming system [10], catalytic pyrolysis of biomass in a two-stage fixed bed reactor system [11], etc. For example, Chaiwatanodom et al. [6] studied the production of syngas from biomass gasification using recycled CO₂ from the process as a gasifying agent by process modelling using the Aspen Plus program. The authors showed that the ratio of syngas production was varied depending upon amount of CO₂ fed into the system, gasification temperature, and pressure. Waheed et al. [12] studied the production of hydrogen from biochar derived from sugar cane bagasse pyrolysis via steam catalytic gasification. Type of catalyst, gasification temperature, and steam flow rate were found to affect hydrogen yield.

Although biomass gasification has been proven to be one of the most efficient techniques for syngas production, one drawback of this technique is the production of CO₂ in the product stream [13–16]. As is known, the release of CO₂ is a cause of the greenhouse gas effect; storage or utilization of CO₂ has therefore attracted interest worldwide. In our previous work [7], utilization of the released CO₂ as a co-gasifying agent has been investigated for combined gasification with the steam reforming process via thermodynamic analysis using the Aspen Plus program. The results showed that the use of CO₂ recycled from a separation process as a co-gasifying agent could enhance coal gas efficiency and reduce CO₂ emissions. However, syngas composition was obtained differently depending upon combination pattern as well as reforming temperature and feed ratio; separation of CO₂ after gasification process offered a higher H₂/CO ratio when compared with the system that extracted CO₂ after the reforming process. Higher reforming temperature and H₂O feed can lead to higher production of H₂. In this work, the combination of biochar gasification and the reforming process for syngas production is experimentally investigated using a packed-bed reactor system. Effects of combination pattern, operating temperature, feed ratio of gasifying agent, and amount of catalyst on syngas production and CO₂ emission are examined. In addition, we have applied the concept of sorption-enhanced steam reforming by using a one-body multi-functional material, which contains CO₂ sorbent and catalyst, to the reforming system with the purpose on improving process efficiency.

2. Materials and Methods

2.1. Material Synthesis

In this work, 12.5 wt.% of Ni on a γ -Al₂O₃ support was used as reforming catalyst, as it has been proven that it is suitable for steam reforming [17]. The material was prepared by the wet impregnation method using Ni(NO₃)₂·6H₂O as precursor. Firstly, 6.66 g of Ni(NO₃)₂·6H₂O was dissolved in 80 mL of deionized water, then 17.87 g of γ -Al₂O₃ was added into aqueous nickel nitrate solution and stirred at 80 °C until the water was almost completely evaporated. The solid was dried at 120 °C overnight and calcined at 600 °C for 3 h in air.

CaO on Al₂O₃ support, named CaO/Ca₁₂Al₁₄O₃₃, was used as CO₂ adsorbent as it offers high CO₂ sorption capacity in the temperature range of steam reforming [18]. In this work, CaO/Ca₁₂Al₁₄O₃₃ was synthesized by the sol-gel method using Al(NO₃)₃·9H₂O and Ca(NO₃)₂·4H₂O as precursors. To prepare this sorbent, 4.22 g of Ca(NO₃)₂·4H₂O was mixed with 2.31 g of Al(NO₃)₃·9H₂O in DI (deionized) water. Then, 5.02 g of citric acid were added into the solution, which was stirred at 80 °C for 7 h. After that, the mixture was placed at ambient temperature for 18 h to form wet gel. Later, the wet gel was dried at 80 °C for 5 h and at 110 °C for 12 h, respectively, followed by calcination at 850 °C for 2 h under dried air. At this stage, CaO/Ca₁₂Al₁₄O₃₃ containing CaO:Ca₁₂Al₁₄O₃₃ = 70:30 wt.% was obtained.

One-body multi-functional sorbent/catalyst material, designated as xwt.% NiO/CaO-Ca₁₂Al₁₄O₃₃, was prepared by sol-gel method following Changjun et al. [19]. In brief, 3.11 g of Ni(NO₃)₂·6H₂O, 5.69 g of Al(NO₃)₃·9H₂O, and 17.81 g of Ca(NO₃)₂·4H₂O, were dissolved in 109 mL of DI water with the addition of citric acid using a molar ratio of citric acid to Al³⁺, Ni²⁺, Ca²⁺ equal to 1.2:1:1:1. The solution was adjusted to pH 1–2 by nitric acid. Then, the solution was heated up and stirred at

80 °C under reflux for 2 h. After that, ethylene glycol (mass ratio polyethylene glycol to citric acid of 0.5) was added into the solution, and stirred under reflux at 105 °C for 5 h. The solution was thereafter dried in an oven at 110 °C for 12 h and calcined at 850 °C for 2 h under dried air.

2.2. Material Characterization

Synthetic materials were characterized their compositions and crystallinity by the X-ray diffraction (XRD) technique; Bruker model D8 Advance (Bruker Crop., Billerica, MA, USA). Surface area, pore size, and pore volume were investigated by N₂ adsorption/desorption isotherm by Brunauer–Emmett–Teller (BET) technique; Micromeritics model 3Flex (Micromeritics Instrument Corp., Norcross, GA, USA). Morphologies of the samples were determined by a scanning electron microscope (SEM); Hitachi model S-3400N (Hitachi High-Technologies Corp., Tokyo, Japan).

2.3. Syngas Production Test

Syngas production experiments were carried out by using two-connected fixed-bed reactors, one for biomass gasification and the other for reforming reaction (see Figure 1). Prior to running experiment, biochar was pretreated by Ar with a flow rate of 50 mL/min at 600 °C for 60 min. Sorbent and catalyst materials were pretreated by Ar with a flow rate of 50 mL/min at 850 °C for 30 min followed by the same flow rate of H₂ at 850 °C for 30 min, respectively. In this work, gasification temperature was varied between 850 °C and 950 °C and that of reforming was varied between 500 °C and 650 °C under atmospheric pressure. The gasifying agent was fed at a fixed ratio of O₂ and C, whereas CO₂ and H₂O were varied. The CO₂/O₂/H₂O/C feed ratios were varied in the range of 0–0.5:0.125:0–1.5:1. All experiments were carried out by fixing total feed flow rate to yield gas hourly space velocity (GHSV) ca. 700 h⁻¹.

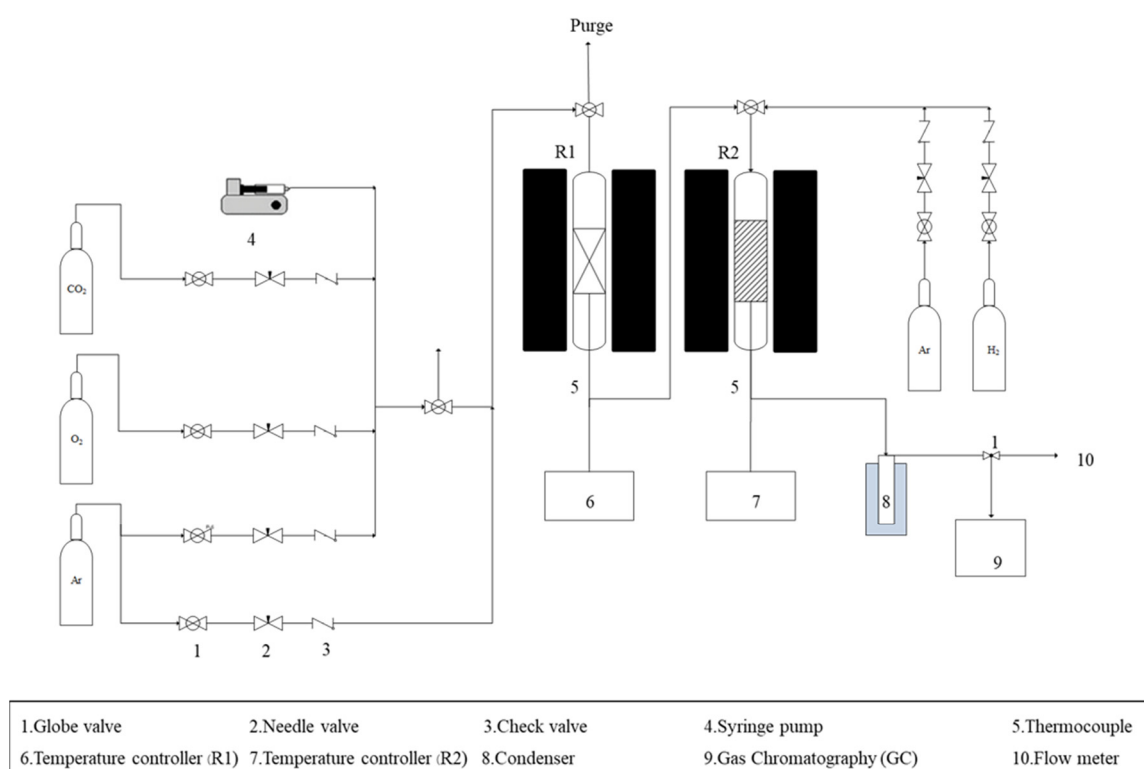


Figure 1. Schematic diagram of experimental setup for syngas production.

Performances of the combined process were determined in terms of biochar conversion (%Biochar conversion), ratio of H₂/CO in the produced syngas (H₂/CO ratio), and CO₂ emission ratio (CO₂ EMR) as defined as follows:

%Biochar conversion:

$$\% \text{Biochar conversion} = \frac{\text{mole of biochar}_{\text{in}} - \text{mole of biochar}_{\text{out}}}{\text{mole of biochar}_{\text{in}}} \times 100 \quad (1)$$

H₂/CO ratio:

$$\text{H}_2/\text{CO ratio} = \frac{\text{mole of H}_2 \text{ produced}}{\text{mole of CO produced}} \quad (2)$$

CO₂ emission ratio, CO₂ EMR:

$$\text{CO}_2 \text{ emission ratio (CO}_2 \text{ EMR)} = \frac{\text{mole of CO}_2 \text{ emission from CO}_2 \text{ outlets}}{\text{mole of CO}_2 \text{ total}} \quad (3)$$

where CO₂ total is the amount of CO₂ produced from the gasifier.

3. Results and Discussions

3.1. Effect of Gasification Temperature

Conversion of biochar was firstly investigated by studying the effect of gasification temperature using H₂O and O₂ as gasifying agents with a H₂O:O₂:C feed molar ratio of 0.25:0.25:1. As shown in Figure 2, high biochar conversions of 97.5%, 98.7%, and 98.1% could be obtained by gasification at temperatures of 850 °C, 900 °C, and 950 °C, respectively. The results confirm that this temperature range is suitable for biochar gasification.

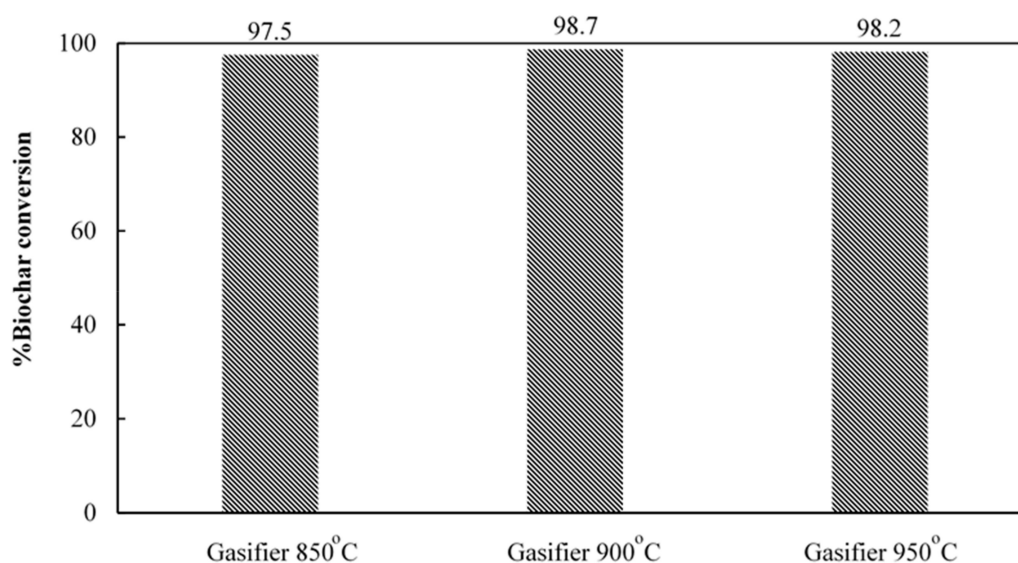
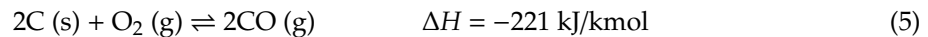


Figure 2. %Biochar conversion at different gasification temperatures using a H₂O:O₂:C feed molar ratio of 0.25:0.25:1.

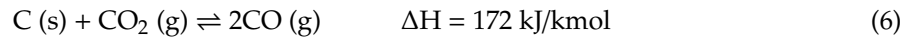
Product compositions obtained from the gasifier at different temperatures are shown in Figure 3. For the range of gasification temperature investigated in this work, two main products, CO and CO₂, are obtained. The obtained products could be due to the water-gas reaction (Equation (4)) and the partial oxidation reaction (Equation (5)).

Water gas reaction



Partial oxidation reaction

Increasing gasification temperature from 850 °C to 950 °C shows insignificant effects on the production of H₂, whereas a gradual increase of CO production is observed with the reduction of CO₂. This phenomenon could be attributed to the result of a favorable Boudouard reaction (Equation (6)) [12,20]:

Boudouard reaction

As seen from the above results, very small amounts of hydrogen can be obtained with solely biochar gasification. As a consequence, upgrading hydrogen production would further investigated by combining with steam reforming reaction. For gasification reaction, it was shown that almost complete conversion of biochar can be obtained in the range of gasification temperature investigated in this work, 850 °C to 950 °C. For optimistic reasons, a gasification temperature of 900 °C was chosen for investigating other effects on syngas production.

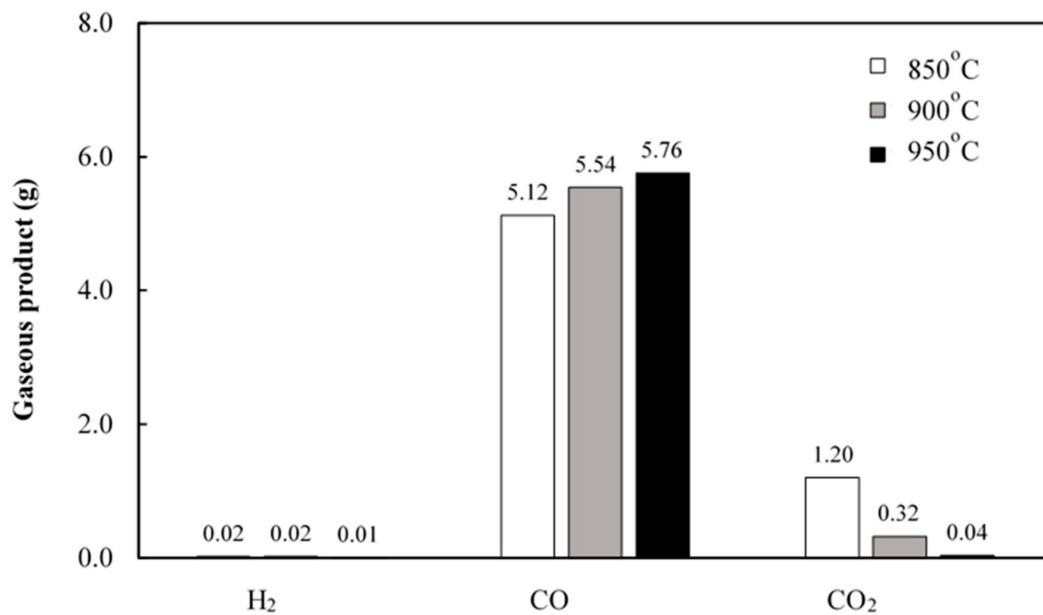


Figure 3. Gasification of biochar at different gasification temperatures (H₂O:O₂:C feed molar ratio of 0.25:0.25:1 under atmospheric pressure).

3.2. Effect of Combined Gasification and Reforming Reaction

As shown in the previous section, biochar gasification can yield insignificant amount of H₂, to enhance the production of H₂, reforming reactor was introduced into the gasification system. In this investigation, to prove the concept of our simulation works [7] and to introduce process integration concept, three different packing patterns of sorbent and catalyst were studied, as shown in Figure 4. In Figure 4a, the catalyst and the sorbent were packed separately and the catalyst was packed on top of the sorbent, designated as the combined biomass gasifier and water-gas shift with Post-CO₂ recycle (CBGR-PostCO₂). In Figure 4b, the sorbent was placed on top of the catalyst, designated as the combined biomass gasifier and water-gas shift with Pre-CO₂ recycle (CBGR-PreCO₂), and in Figure 4c the developed one-body of combined catalyst with sorbent was introduced into the system, designated as the combined biomass gasifier and water-gas shift with multifunctional-CO₂ recycle (CBGR-SimulCO₂). In order to utilize CO₂, in this section, CO₂ was also used as co-gasifying agent

together with H_2O and O_2 . In this work, performances of each combined system were investigated in terms of syngas production and CO_2 emission ratio at a fixed gasification temperature of $900\text{ }^\circ\text{C}$, reforming temperature of $600\text{ }^\circ\text{C}$, $H_2O:CO_2:O_2:C$ feed molar ratio of 0.5:0.5:0.125:1, and NiO content of 12.5 wt.%.

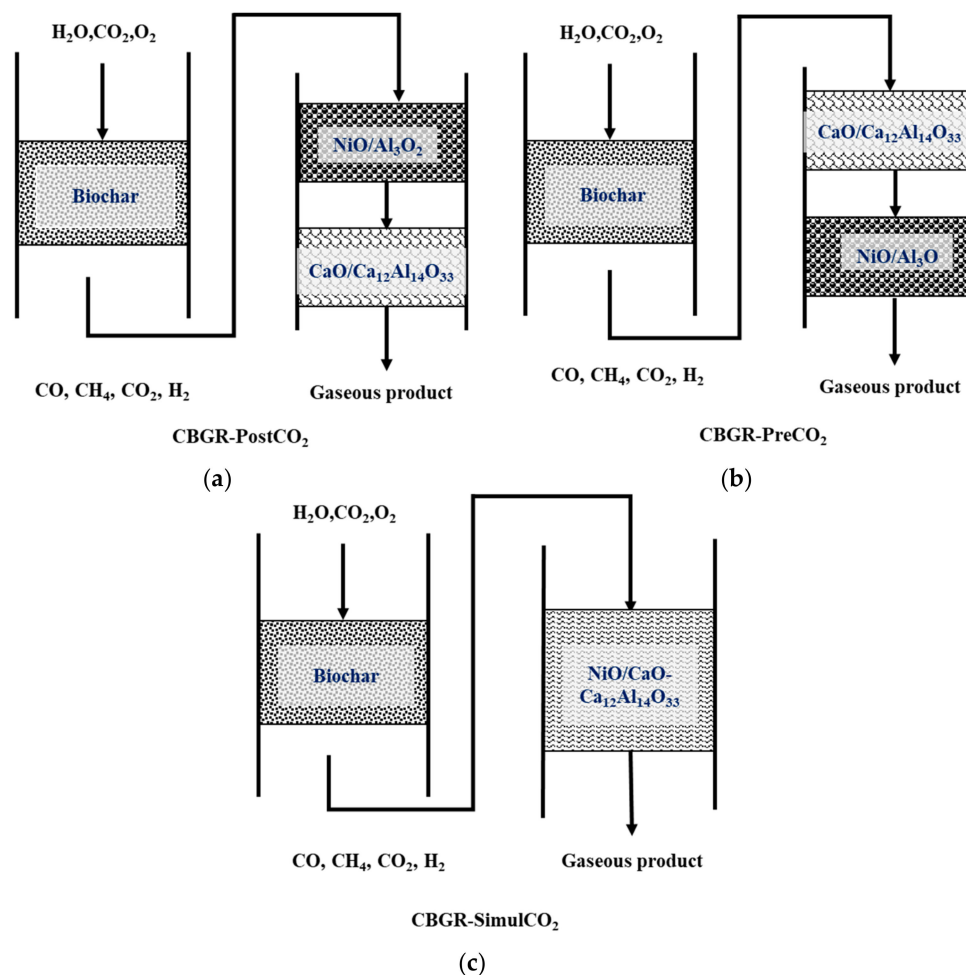


Figure 4. Patterns of sorbent and catalyst packing in the water–gas shift reactor (a) CBGR-PostCO₂, (b) CBGR-PreCO₂, and (c) CBGR-SimulCO₂.

Prior to running experiments, compositions of biochar were determined by proximate and ultimate analysis (Table 1). Compositions and surface textural properties of the synthetic materials were examined by XRD (Figure 5) and BET surface area analysis (Table 2), respectively. The results show XRD peaks corresponding to CaO at $2\theta = 32.204, 37.347,$ and 64.154 , Ca₁₂Al₁₄O₃₃ at $2\theta = 18.052, 54.972,$ and 62.634 , and NiO at $2\theta = 37.249, 43.297, 62.934,$ and 67.271 [17,21]. Note that Ca(OH)₂ peaks, which are assigned at $2\theta = 28.672, 34.102,$ and 47.121 , are observed in the XRD pattern due to the fact that CaO is a hygroscopic material. The BET surface area of 12.5 wt.% NiO/CaO-Ca₁₂Al₁₄O₃₃ is $13.5\text{ m}^2/\text{g}$, that of CaO-Ca₁₂Al₁₄O₃₃ is $5.91\text{ m}^2/\text{g}$, and that of 12.5 wt.% NiO/Al₂O₃ is $59.1\text{ m}^2/\text{g}$, respectively.

Table 1. Proximate and ultimate analysis results of biochar.

Proximate (wt.%)		Ultimate (wt.%)	
Moisture	5.30	C	80.20
Volatile matters	36.26	H	2.83
Fixed carbon	56.40	O (balance)	16.39
Ash	2.05	N	0.58

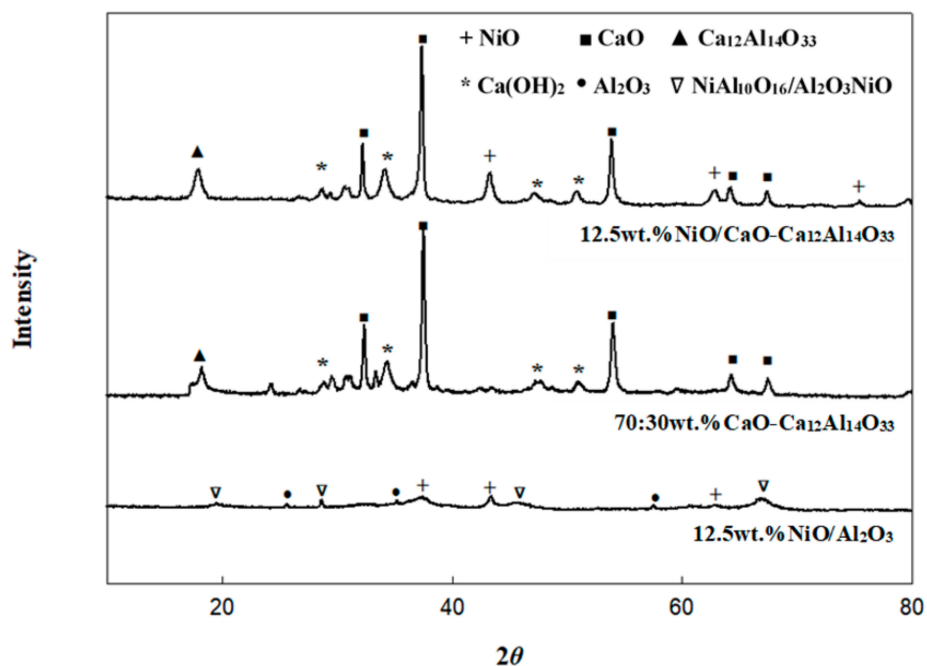


Figure 5. XRD patterns of NiO/Al₂O₃, CaO/Ca₁₂Al₁₄O₃₃, and 12.5 wt.% Ni/CaO-Ca₁₂Al₁₄O₃₃.

Table 2. Physical properties of materials from BET measurements.

Sample	Surface Area (m ² /g)	Pore Volume (cm ³ /g)	Pore Size (nm)
12.5 wt.% NiO/Al ₂ O ₃	59.1	0.150	0.09
CaO-Ca ₁₂ Al ₁₄ O ₃₃	5.91	0.009	0.13
12.5 wt.% NiO/CaO-Ca ₁₂ Al ₁₄ O ₃₃	13.5	0.016	0.16

As shown in Figure 6, the addition of reforming system (regardless of combination pattern) can provide higher H₂ production when compared with solely gasification reaction shown in Section 3.1. This could be due to the result of water–gas shift reaction (Equation (7)), where the main gasification product, CO, is further reacted with steam to form H₂ and CO₂ in the steam reforming reactor.

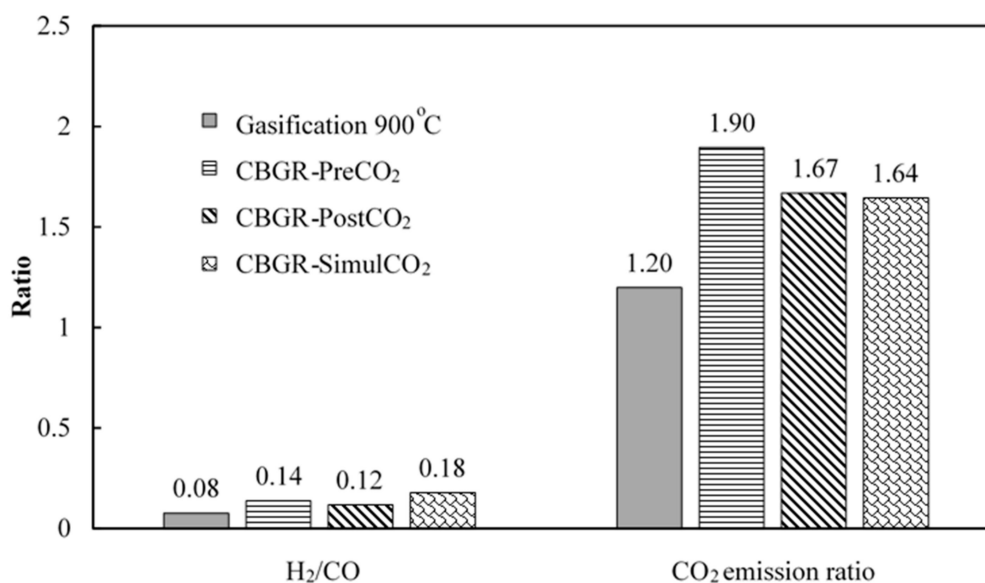


Figure 6. H₂/CO and CO₂ emission ratio from different proposed systems (H₂O:CO₂:O₂:C feed molar ratio of 0.5:0.5:0.125:1, gasification at 900 °C, reforming at 600 °C and ambient pressure).

Water–gas shift reaction

Combining gasification with reforming system in different patterns shows the effect on syngas production and CO₂ emission ratio as demonstrated in Figure 6. The CBGR-PreCO₂ offers higher H₂ than the CBGR-PostCO₂, which is in good agreement with our simulation results proposed previously [7]. The enhancement of H₂ is believed to be mainly due to the result of the water–gas shift reaction. For the CBGR-PreCO₂ system, CO₂ was removed from the system prior to the water–gas shift reaction, leading to a favorable forward water–gas shift reaction. On the other hand, the CO₂ emission from CBGR-PreCO₂ is higher than CBGR-PostCO₂. This could be because the produced CO₂ is partly adsorbed by CaO-based sorbent in the CBGR-PostCO₂ system. Overall, the CBGR-SimulCO₂ system offers the highest H₂ production when compared with the CBGR-PreCO₂ system and the CBGR-PostCO₂ systems. This observation is due to the effect of the sorption-enhanced water–gas shift reaction; simultaneous removal of CO₂ can overcome the limitation of water–gas shift reaction (SEWGS) by inducing the system to proceed forward according to Le Chatelier’s principle. More interestingly, the CO₂ emission ratio of the CBGR-SimulCO₂ system is found to be minimal, which could be attributed to greater CO₂ sorption capacity as mass transfer is favorable in the case of using one-body multi-functional material.

CO₂ adsorption

As seen above, applying sorption-enhanced reaction (CBGR-SimulCO₂) system by introducing one-body multi-functional material can slightly increase H₂/CO with the reduction of the CO₂ emission from the system when compared with other sorption systems. However, all patterns provide H₂/CO ratios less than 0.18. This might be due to this biochar (H content is 2.83 wt.% from the ultimate analysis result, Table 1) not being favorable as feedstock for the production of syngas containing high hydrogen content. Nevertheless, the effect of operating conditions, including amount of catalyst, sorption-enhanced reaction temperature, and feed ratio of gasifying agent, were investigated for the combined gasification with SEWGS system.

3.3. Effect of Catalyst Amount

In this section, the effect of amount of catalyst on gaseous production, syngas H₂/CO ratio, and CO₂ emission ratio was studied. Figure 7 shows compositions of gaseous product for different wt.% of NiO. Comparative amounts of hydrogen production are obtained for all NiO contents, whereas the maximum of CO production is found with 12.5 wt.% Ni/CaO-Ca₁₂Al₁₄O₃₃. This result could be because the 12.5 wt.% Ni/CaO-Ca₁₂Al₁₄O₃₃ possesses the highest BET surface area, resulting in higher active surface exposure, as shown in Table 3. Large amount of NiO (17.5 wt.%) could block the small pores of the support, leading to the reduction of surface area as well as pore volume with an increase of average pore size diameter. For the 7.5 wt.% Ni/CaO-Ca₁₂Al₁₄O₃₃, small amounts of Ni cannot help prevent the agglomeration of CaO particles, resulting in lower surface area (Table 3) and dense packing particles (Figure 8).

Table 3. Physical properties of multi-functional materials for different NiO contents.

Sample	Surface Area (m ² /g)	Pore Volume (cm ³ /g)	Pore Size (nm)
7.5 wt.% NiO/CaO-Ca ₁₂ Al ₁₄ O ₃₃	11.70	0.026	0.11
12.5 wt.% NiO/CaO-Ca ₁₂ Al ₁₄ O ₃₃	13.50	0.016	0.16
17.5 wt.% NiO/CaO-Ca ₁₂ Al ₁₄ O ₃₃	12.45	0.023	0.11

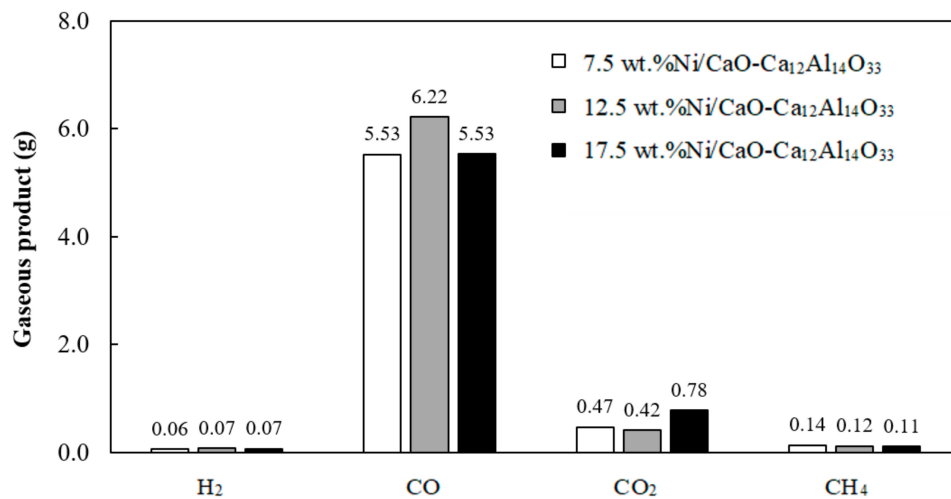


Figure 7. Product composition at different wt.% of Ni on Ni/CaO-Ca₁₂Al₁₄O₃₃ using a H₂O:CO₂:O₂:C feed molar ratio of 0.5:0.1:0.125:1, gasification at 900 °C, and sorption-enhanced water–gas shift reaction (SEWGS) at 600 °C.

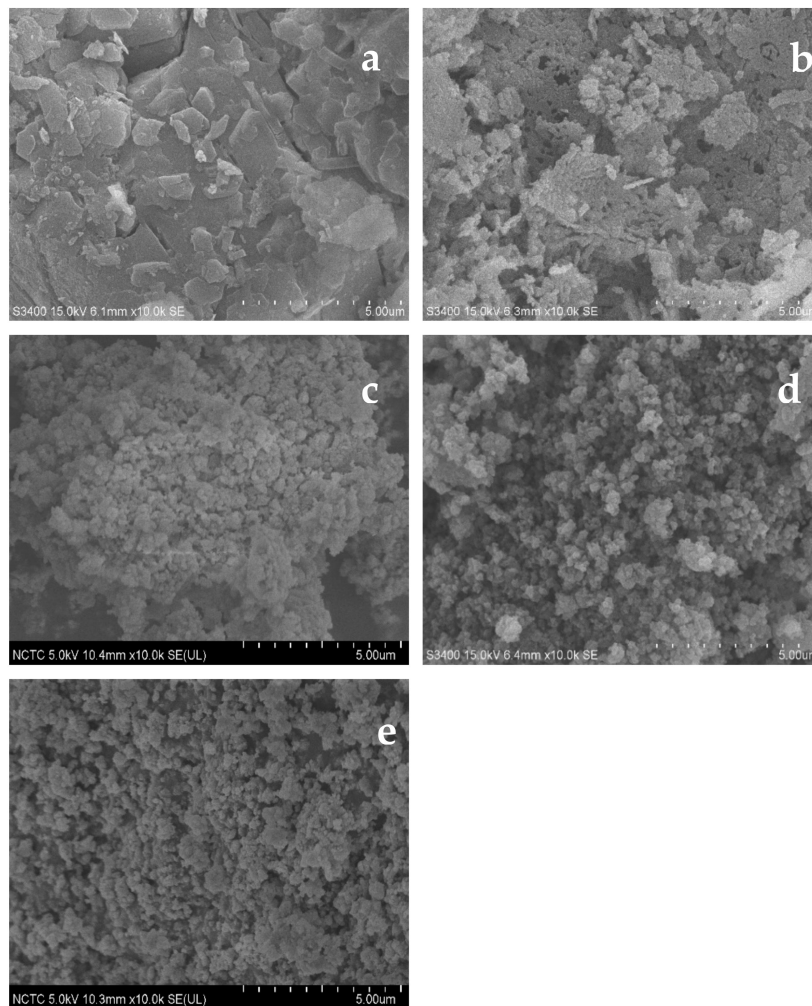


Figure 8. SEM images of fresh sample materials; (a) Ni/Al₂O₃, (b) CaO-Ca₁₂Al₁₄O₃₃, (c) 7.5 wt.% Ni/CaO-Ca₁₂Al₁₄O₃₃, (d) 12.5 wt.% Ni/CaO-Ca₁₂Al₁₄O₃₃, and (e) 17.5 wt.% Ni/CaO-Ca₁₂Al₁₄O₃₃.

Figure 9 shows CO₂ emission ratio of different NiO contents. The results show that the 12.5 wt.% Ni/CaO-Ca₁₂Al₁₄O₃₃ provides minimum CO₂ emission ratio, which could be due to the result of high

performance of SEWGS reaction. Lower CO₂ adsorption observed with the 7.5 wt.% Ni/CaO-Ca₁₂Al₁₄O₃₃ and the 17.5 wt.% Ni/CaO-Ca₁₂Al₁₄O₃₃ could be attributed to lower surface area as shown in Table 3.

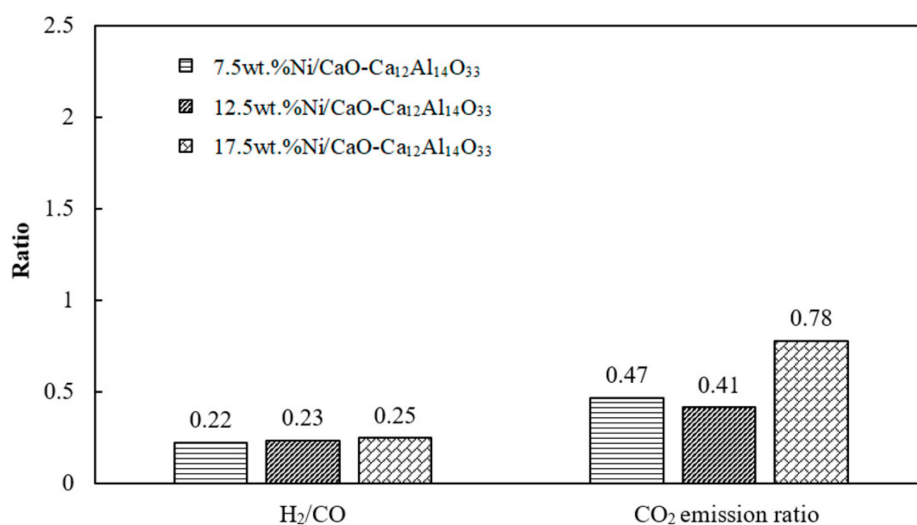


Figure 9. H₂/CO and CO₂ emission ratios at different wt.% of Ni of Ni/CaO-Ca₁₂Al₁₄O₃₃ using a H₂O:CO₂:O₂:C feed molar ratio of 0.5:0.1:0.125:1, gasification at 900 °C, and SEWGS at 600 °C.

3.4. Effect of Sorption-Enhanced Water–Gas Shift (SEWGS) Temperature

As seen from the previous section, combining gasification with SEWGS reaction with the use of 12.5 wt.% Ni/CaO-Ca₁₂Al₁₄O₃₃ can provide greater H₂/CO ratio with lower CO₂ emission. In this section, the effect of SEWGS temperature on H₂/CO ratio and CO₂ emission ratio was investigated. Figure 10 shows product compositions obtained at different SEWGS temperatures. Increasing SEWGS temperature from 500 °C to 650 °C does not affect the production of hydrogen or the quality of syngas, as comparative values are observed. The reduction of CO could be due to the reactions between CO and H₂O (Equation (7)) and CO and H₂ (reversed Equation (9)) which lead to the formation of CH₄. Increasing temperature results in the decrease of CH₄ due to exothermic reaction of Equation (9). The CO₂ emission is found to decrease with increasing SEWGS temperature from 500 to 650 °C (Figure 11). This observation could be due to the result of the suitable CO₂ sorption condition of CaO sorbent at a high temperature of 650 °C [22,23].

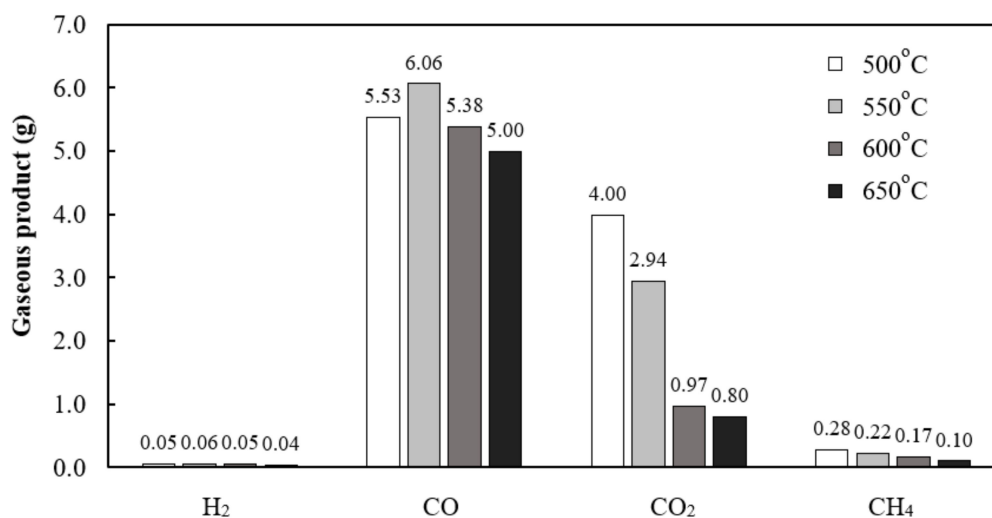


Figure 10. Product composition obtained from different SEWGS temperatures using a H₂O:CO₂:O₂:C feed molar ratio of 0.5:0.5:0.125:1 and gasification at 900 °C.

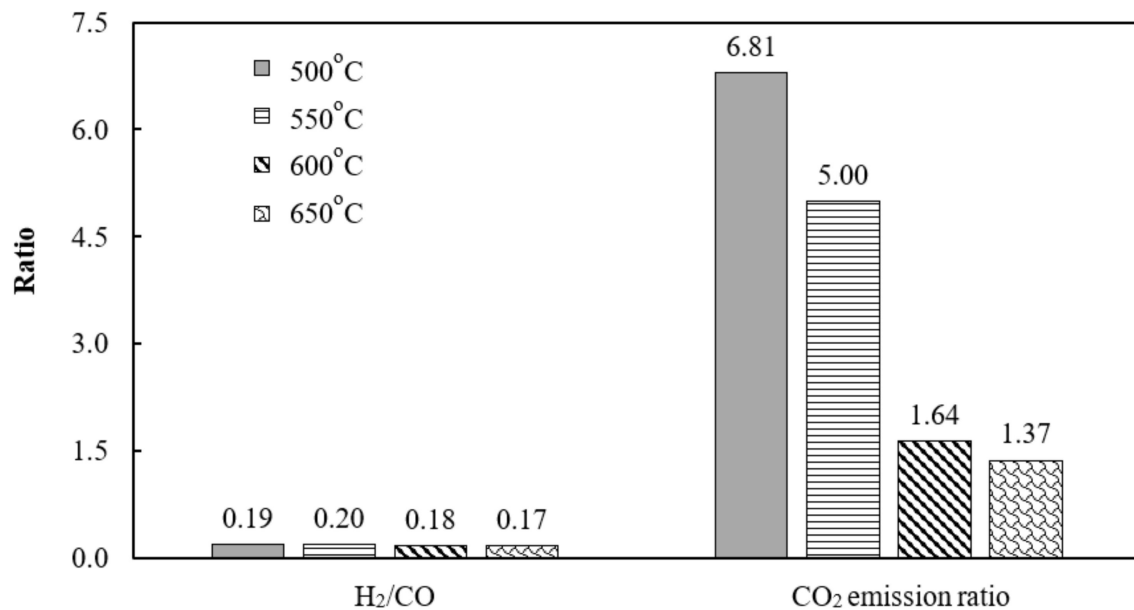


Figure 11. H₂/CO and CO₂ emission ratios at different SEWGS temperatures using a H₂O:CO₂:O₂:C feed molar ratio of 0.5:0.5:0.125:1 and gasification at 900 °C.

CO₂ reforming



3.5. Effect of Gasifying Agent

As the gasifying agent is one factor that can affect gasification of biomass [24], in this work, we investigated the effect of introducing CO₂ as co-gasifying agent in order to utilize the CO₂. The feed molar ratio of co-feed gasifying agent was fixed at H₂O:O₂:C = 0.5:0.125:1, while the CO₂/C molar ratio was varied between 0.1 and 0.5:1 using 12.5 wt.% Ni/CaO-Ca₁₂Al₁₄O₃₃ at a gasification temperature of 900 °C and SEWGS temperature of 600 °C (Section 3.5.1). And effect of H₂O feed as gasifying agent was investigated by varying the H₂O:C ratio between 0.5–1.5:1 at a fixed CO₂:O₂:C feed molar ratio of 0.1:0.125:1, gasification temperature of 900 °C, and SEWGS temperature of 600 °C (Section 3.5.2).

3.5.1. Effect of CO₂ Feed

Figure 12 presents product composition obtained from the reaction with different amounts of CO₂ feed. The results show that CO increases with increasing CO₂/C ratio parallel with an increase of CO₂ emission ratio (Figure 13). This observed result could be attributed to the reverse Boudouard reaction (Equation (1)). It is noted that although higher amounts of H₂ produced from the system could be obtained due to the result of water–gas shift reaction, negligible amounts of produced H₂ are still observed. This result might be because of insufficient steam feed into the system, leading to a smaller contribution of the water–gas shift reaction. Our observation is consistent with the results obtained from a thermodynamic study of lignite coal gasification reported by Kale et al. [25], where an increase of CO₂/C feed mole ratio from 0 to 1 led to a decrease of H₂/CO ratio from 3.04 to 0.7. It is also noted that CH₄ is observed in gaseous products, implying that reverse Boudouard reaction (Equation (1)) could occur due to the addition of CO₂, resulting in higher production of CO which could further react with the produced H₂ to form CH₄ and CO₂ (reversed Equation (9)).

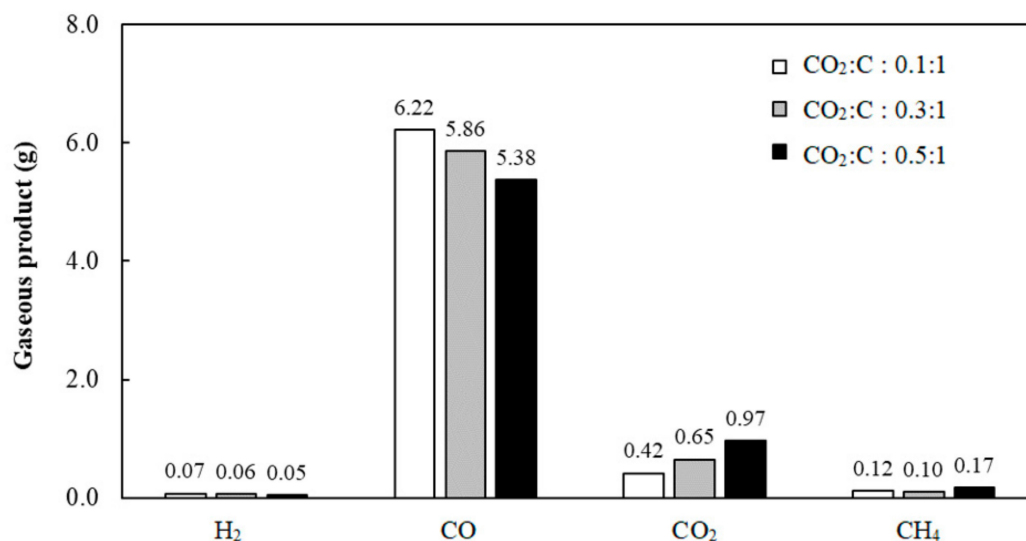


Figure 12. Product composition at different CO₂:C ratios using a H₂O:CO₂:O₂:C feed molar ratio of 0.5:0.1–0.5:0.125:1, gasification at 900 °C, and SEWGS at 600 °C.

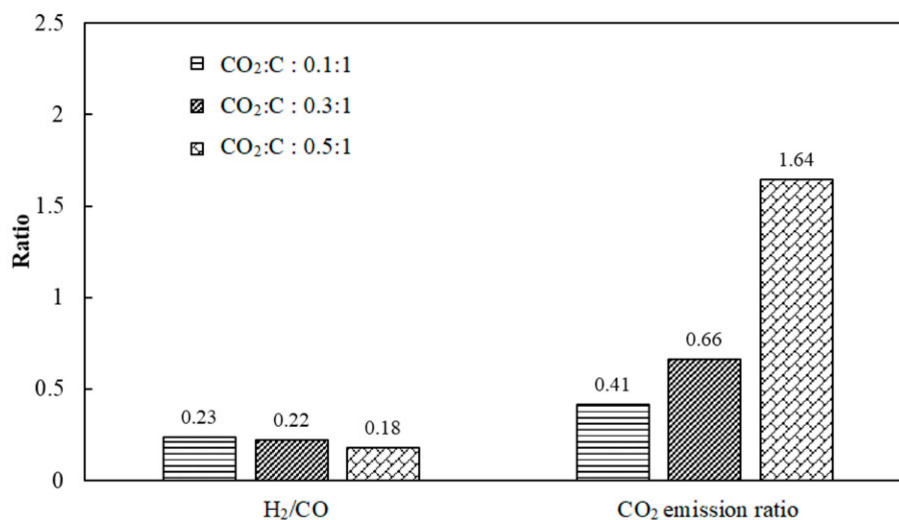


Figure 13. H₂/CO and CO₂ emission ratios at different CO₂:C ratios using a H₂O:CO₂:O₂:C feed molar ratio of 0.5:0.1–0.5:0.125:1, gasification at 900 °C, and SEWGS at 600 °C.

3.5.2. Effect of H₂O Feed

In Figure 14, increasing of H₂O feed is expected to enhance the production of H₂ due to a water gas reaction (Equation (4)) and water–gas shift reaction (Equation (7)); however, insignificant H₂ production is observed. This result might be due to insufficient H₂O feed as discussed previously. Nevertheless, quality of syngas (H₂/CO ratio) is found to increase with increasing H₂O feed (Figure 15). This observation could possibly be due to the produced CO reacting with the produced H₂ via the reversed CO₂ reforming reaction (reversed Equation (9)) as evidenced by the reduction of CO and the increase of CO₂ shown in Figure 14.

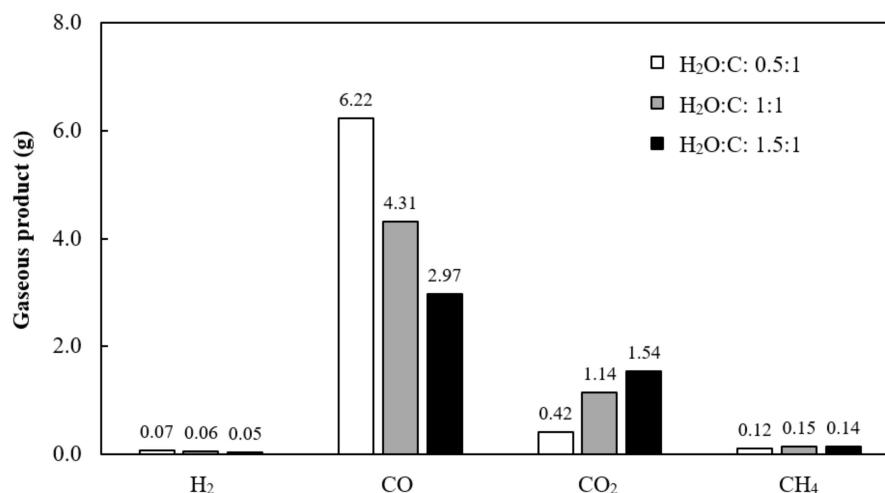


Figure 14. Product composition at different H₂O:C ratios using a H₂O:CO₂:O₂:C feed molar ratio of 0.5–1.5:0.1:0.125:1, gasification at 900 °C and SEWGS at 600 °C.

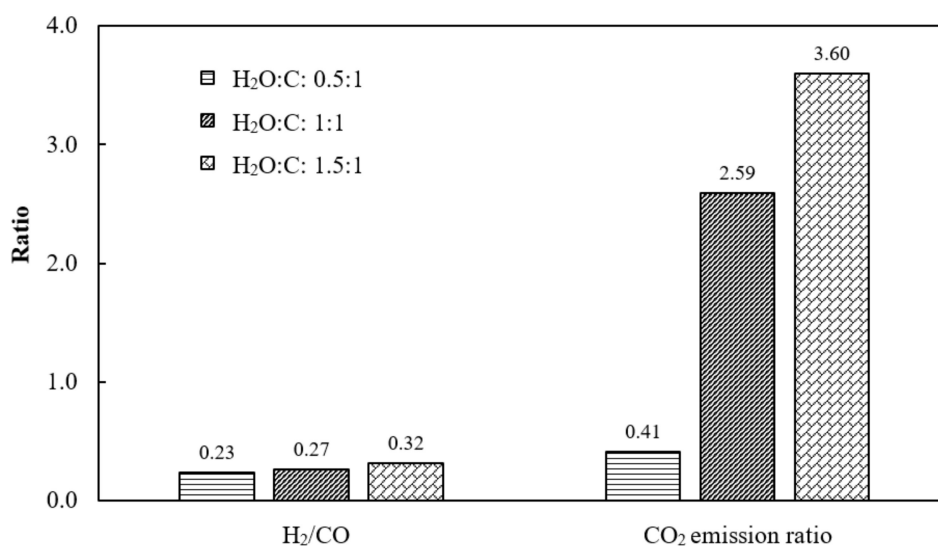


Figure 15. H₂/CO and CO₂ emission ratios at different H₂O:C ratios using a H₂O:CO₂:O₂:C feed molar ratio of 0.5–1.5:0.1:0.125:1, gasification at 900 °C, and SEWGS at 600 °C.

4. Conclusions

Our studies investigated the production of syngas from biochar using the combined gasification and sorption-enhanced water–gas shift reaction. The optimum gasification temperature was 900 °C with a H₂O:O₂:C feed molar ratio of 0.25:0.25:1. The one-body material combining catalyst with sorbent (CBGR-SimulCO₂) could provide the highest H₂/CO ratio as well as the lowest CO₂ emissions when compared to the other systems. In addition, the effect of sorption-enhanced water–gas shift temperature was shown to affect CO₂ emissions. Increasing the operating temperature from 500 to 650 °C led to a decrease of the CO₂ emission ratio. Increasing the CO₂/C ratio from 0.1 to 0.5 resulted in an increase of CO production with a lower CO₂ emission ratio. In addition, increasing the H₂O/C ratio from 0.5 to 1.5 provided higher syngas production, with H₂/CO ratios of 0.23 and 0.32, respectively.

Author Contributions: Conceptualization, Supawat Vivanpatarakij; Data curation, Supanida Chimpae, Suwimol Wongsakulphasatch, Supawat Vivanpatarakij and Fasai Wiwatwongwana; Formal analysis, Suwimol Wongsakulphasatch, Supawat Vivanpatarakij, Thongchai Glinrun and Weerakanya Maneepkorn; Funding acquisition, Suttichai Assabumrungrat; Investigation, Supanida Chimpae and Thongchai Glinrun; Methodology, Supanida Chimpae, Suwimol Wongsakulphasatch and Supawat Vivanpatarakij; Project administration, Suttichai Assabumrungrat; Resources, Thongchai Glinrun, Fasai Wiwatwongwana and

Weerakanya Maneeprakorn; Supervision, Suwimol Wongsakulphasatch, Supawat Vivanpatarakij and Suttichai Assabumrungrat; Validation, Thongchai Glinrun and Weerakanya Maneeprakorn; Writing—original draft, Supanida Chimpae, Suwimol Wongsakulphasatch, Supawat Vivanpatarakij and Suttichai Assabumrungrat.

Funding: The authors would like to acknowledge funding support from the Ratchadapisek Sompoch Endowment Fund 2016 of Chulalongkorn University (CU-59-003-IC), and King Mongkut's University of Technology North Bangkok (contract no. KMUTNB-KNOW-61-029). S.W. and S.A. also wish to acknowledge the "Research Chair Grant" of the National Science and Technology Development Agency (NSTDA).

Conflicts of Interest: The authors declare no conflict of interest.

References

- Rodrigues, M.; Faaij, A.P.C.; Walter, A. Technol-economic analysis of co-fired biomass integrated gasification/combined cycle systems with inclusion of economies of scale. *Energy* **2003**, *28*, 1229–1258. [[CrossRef](#)]
- Hamelinck, C.N.; Faaij, A.P.C.; den Uil, H.; Boerrigter, H. Production of FT transportation fuels from biomass; technical options, process analysis and optimization, and development potential. *Energy* **2004**, *29*, 1743–1771. [[CrossRef](#)]
- Adams, T.A.; Hoseinzade, L.; Madabhushi, P.B.; Okeke, I.J. Comparison of CO₂ capture approaches for fossil-based power generation: Review and Meta-study. *Processes* **2017**, *5*, 44. [[CrossRef](#)]
- Acharya, B.; Dutta, A.; Basu, P. Chemical-looping gasification of biomass for hydrogen-enriched gas production with in-process carbon dioxide capture. *Energy Fuels* **2009**, *23*, 5077–5083. [[CrossRef](#)]
- Pang, Y.; Hammer, T.; Müller, D.; Karl, J. Investigation of nonthermal plasma assisted charcoal gasification for production of hydrogen-rich syngas. *Processes* **2019**, *7*, 114. [[CrossRef](#)]
- Chaiwatanodom, P.; Vivanpatarakij, S.; Assabumrungrat, S. Thermodynamic analysis of biomass gasification with CO₂ recycle for synthesis gas production. *Appl. Energy* **2014**, *14*, 10–17. [[CrossRef](#)]
- Kraisornkachit, P.; Vivanpatarakit, S.; Amornraksa, S.; Simasatitkul, L.; Assabumrungrat, S. Performance evaluation of different combined systems of biochar gasifier, reformer and CO₂ capture unit for synthesis gas production. *Int. J. Hydrog. Energy* **2016**, *41*, 13408–13418. [[CrossRef](#)]
- Ma, Z.; Zhang, S.; Xie, D.; Yan, Y. A novel integrated process for hydrogen production from biomass. *Int. J. Hydrog. Energy* **2014**, *39*, 1274–1279. [[CrossRef](#)]
- Waheed, Q.M.K.; Williams, P.T. Hydrogen production from high temperature pyrolysis/steam reforming of waste biomass: Rice husk, sugar cane bagasse, and wheat straw. *Energy Fuels* **2013**, *27*, 6695–6704. [[CrossRef](#)]
- Gao, N.; Lia, A.; Quan, C.; Gao, F. Hydrogen-rich gas production from biomass steam gasification in an updraft fixed-bed gasifier combined with a porous ceramic reformer. *Int. J. Hydrog. Energy* **2008**, *33*, 5430–5438. [[CrossRef](#)]
- Liu, S.; Zhu, J.; Chen, M.; Xin, W.; Yang, Z.; Kong, L. Hydrogen production via catalytic pyrolysis of biomass in a two-stage fixed bed reactor system. *Int. J. Hydrog. Energy* **2014**, *39*, 13128–13135. [[CrossRef](#)]
- Waheed, Q.M.K.; Wu, C.; Williams, P.T. Hydrogen production from high temperature steam catalytic gasification of bio-char. *J. Energy Inst.* **2016**, *89*, 222–230. [[CrossRef](#)]
- Song, C.; Liu, Q.; Ji, N.; Deng, S.; Zhao, J.; Li, Y.; Song, Y. Alternative pathways for efficient CO₂ capture by hybrid processes—A review. *Renew. Sustain. Energy Rev.* **2018**, *82*, 215–231. [[CrossRef](#)]
- La Villetta, M.; Costa, M.; Massarotti, N. Modelling approaches to biomass gasification: A review with emphasis on the stoichiometric method. *Renew. Sustain. Energy Rev.* **2017**, *74*, 71–88. [[CrossRef](#)]
- Indrawan, N.; Thapa, S.; Bhoi, P.R.; Huhnke, R.L.; Kumar, A. Engine power generation and emission performance of syngas generated from low-density biomass. *Energy Convers. Manag.* **2017**, *148*, 593–603. [[CrossRef](#)]
- Ruiz, J.A.; Juárez, M.C.; Morales, M.P.; Muñoz, P.; Mendivil, M.A. Biomass gasification for electricity generation: Review of current technology barriers. *Renew. Sustain. Energy Rev.* **2013**, *18*, 174–183. [[CrossRef](#)]
- Guohui, L.; Linjie, H.; Josephine, M.H. Comparison of reducibility and stability of alumina-supported Ni catalysts prepared by impregnation and co-precipitation. *Appl. Catal. A* **2006**, *301*, 16–24.
- Cong, L.; Ying, Z.; Ning, D.; Chuguang, Z. Enhanced cyclic stability of CO₂ adsorption capacity of CaO-based sorbents using La₂O₃ or Ca₁₂Al₁₄O₃₃ as additives. *Korean J. Chem. Eng.* **2011**, *28*, 1042–1046.
- Changjun, Z.; Zhiming, Z.; Cheng, Z.; Fang, X. Sol-gel-derived, CaZrO₃-stabilized Ni/CaO-CaZrO₃ bifunctional catalyst for sorption-enhanced steam methane reforming. *Appl. Catal. B* **2016**, *196*, 16–26.

20. Howaniec, N.; Smolinski, A.; Stanczyk, K.; Pichlak, M. Steam co-gasification of coal and biomass derived chars with synergy effect as an innovative way of hydrogen-rich gas production. *Int. J. Hydrog. Energy* **2011**, *36*, 14455–14463. [[CrossRef](#)]
21. Pan, X.; Miaomiao, X.; Zhenmin, C.; Zhiming, Z. CO₂ capture performance of CaO-based sorbents prepared by a pol-gel method. *Ind. Eng. Chem. Res.* **2013**, *52*, 12161–12169.
22. Lu, H.; Reddy, E.P.; Smirniotis, P.G. Calcium oxide based sorbents for capture of carbon dioxide at high temperatures. *Ind. Eng. Chem. Res.* **2006**, *45*, 3944–3949. [[CrossRef](#)]
23. Yu, C.H.; Huang, C.H.; Tan, C.S. A review of CO₂ capture by absorption and adsorption. *Aerosol Air Qual. Res.* **2012**, *12*, 745–769. [[CrossRef](#)]
24. Buttermann, H.C.; Castaldi, M.J. CO₂ as a carbon neutral fuel source via enhanced biomass gasification. *Environ. Sci. Technol.* **2009**, *43*, 9030–9037. [[CrossRef](#)] [[PubMed](#)]
25. Kale, G.R.; Kulkarni, B.D.; Chavan, R.N. Combined gasification of lignite coal: Thermodynamic and application study. *J. Taiwan Inst. Chem. Eng.* **2013**, *45*, 163–173. [[CrossRef](#)]



© 2019 by the authors. Licensee MDPI, Basel, Switzerland. This article is an open access article distributed under the terms and conditions of the Creative Commons Attribution (CC BY) license (<http://creativecommons.org/licenses/by/4.0/>).